Resolution enhancement and separation of reverberation from target echo with the time reversal operator decomposition

Thomas Folégot[a)]
Atlantide, Technopôle Brest-Iroise, BP 80802, 29608 Brest Cedex, France

Claire Prada and Mathias Fink
Laboratoire Ondes et Acoustique, ESPCI, 10, rue Vauquelin, 75005 Paris, France

Time reversal operator (TRO) decompositions are performed in a model of an ocean wave guide containing a target and having different kinds of bottom. The objective is to study the effects of bottom reverberation and absorption by means of ultrasonic experiments. It is shown experimentally that the echo from a target can be separated from the bottom reverberation. Reverberation eigenvectors are back propagated in the wave guide leading to focus on the bottom. An amplitude correction is applied to both reverberation and signal eigenvectors to compensate for bottom absorption and thus to improve target resolution. © *2003 Acoustical Society of America.* [DOI: 10.1121/1.1571541]

I. INTRODUCTION

Time reversal techniques have been demonstrated in ultrasonics[1] and underwater acoustics environments.[2–4] A technique resulting from the analysis of the iterative time reversal process[5] has been developed: the DORT (French acronym for ''Decomposition of the Time Reversal Operator'') method is a scattering analysis technique using a source receiver array (SRA).[6,7] This technique shares some of the principles used in eigenvector decomposition techniques for passive source detection.[8,9] These latter techniques however, assume statistically uncorrelated sources and require the averaging of the measured data, whereas the time reversal operator (TRO) decomposition is an active and deterministic method. It was applied to achieve multitarget detection and selective focusing on point like scatterers through heterogeneous media and specifically in an ideal water wave guide with a perfectly rigid bottom. Taking advantage of the multiple reflection at the wave-guide interfaces, the method allows a large improvement in spatial resolution. The super resolution is used to separate the signal coming from close scatterers and then to focus a wave field at any one of them.[10] This procedure has also been simulated in a Pekeris wave guide.[11–13] More recently, Lingevitch *et al.*[14] showed, by a numerical study, that the method can be applied to reverberation signals in order to achieve focusing on the bottom of the wave guide and thus to increase the focused signal level.

The objective of this paper is to describe the consequences of losses and reverberation in the medium, and to show how these effects can be overcome. Thus, three increasingly complex kinds of horizontal bottoms are used in the experiments to reach a more realistic model of an ocean wave guide than the previous ideal configuration (Fig. 1). The first is a steel bottom interface, which induces neither losses nor reverberation and has a very high critical angle.

The second is a horizontal Plexiglas plate, which induces absorption and has a low critical angle. Finally, a steel plate covered with a continuous sandy layer is used as the third kind of bottom, which induce reverberation.

The DORT method is first applied to the detection of the targets in presence of bottom absorption, which breaks the time reversal invariance. An amplitude compensation technique is proposed in order to increase the signal to noise ratio at the target while back-propagating the eigenvectors. The benefits of this method, in terms of resolution and signal to noise ratio are evaluated with ultrasonic shallow water experiments.

The effect of noise and reverberation is then studied in the realistic sandy wave-guide model. New eigenvalues appear and their physical meaning is analyzed. After amplitude compensation, the corresponding eigenvector is used in the experiment to focus back on the bottom.

II. GENERALIZED FORMULATION OF TRO DECOMPOSITION

The acoustic configuration consists of a number of targets and a vertical SRA of N transducers in a time invariant medium. Authors[6,7,10,11,14] usually construct the TRO by the direct measurement of the interelement impulse functions $k_{i,j}(t)$ and then Fourier transform these functions to provide the array response matrix $\mathbf{K}(\omega)$. In fact, as already shown by Lingevitch,[14] a more general method consists in emitting signals at the same time by the whole transducers set. It increases up to N times the source level of the system. $\mathbf{K}(\omega)$ can then be measured with any chosen orthogonal family of N signals $\mathbf{E_H}(\omega)$ defined by

$$\sum_{m=1,N} E_{i,m}(\omega)E_{j,m}(\omega) = \delta_{i,j}, \quad 1 \leq i,j \leq N, \tag{1}$$

$\mathbf{R}(\omega) = \mathbf{K}(\omega)\mathbf{E_H}(\omega)$ is a measure of the transfer matrix in the same basis as previously but using another basis of emission. The knowledge of $\mathbf{R}(\omega)$ gives $\mathbf{K}(\omega) = \mathbf{R}(\omega)\mathbf{E_H}(\omega)^{-1}$.

_____
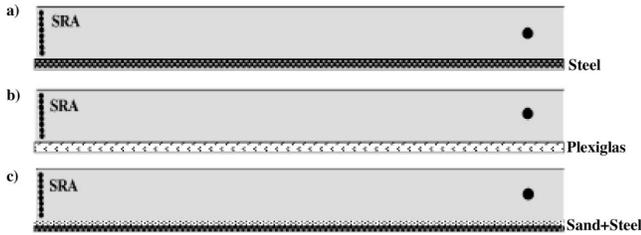[a)]Electronic mail: thomas.folegot@ago.fr

FIG. 1. Three kinds of bottom used for the ultrasonic experiments: (a) Perfectly rigid steel bottom, (b) absorbing Plexiglas bottom, and (c) absorbing and reverberating sand on steel bottom.

To reduce acquisition time and data size, only a subset of M vectors of $\mathbf{E_H}(\omega)$ need be used. As long as M remains much larger than the number of targets in the medium, $\mathbf{R}(\omega)$ provides a good approximation of $\mathbf{K}(\omega)$. The TRO was defined as $\mathbf{K}^\dagger(\omega)\cdot\mathbf{K}(\omega)^6$, where $[\ ]^\dagger$ denotes the complex conjugate transpose. It is a Hermitian matrix which is diagonalizable at all frequencies.[5,6] Nevertheless, in practice, it is convenient to calculate the singular value decomposition of the transfer matrix, possibly after matched filtering,

$$\mathbf{K}(\omega)=\mathbf{U}(\omega)\mathbf{S}(\omega)\mathbf{V}^\dagger(\omega). \qquad (2)$$

$\mathbf{S}(\omega)$ is a real diagonal matrix of the singular values, and $\mathbf{U}(\omega)$ and $\mathbf{V}(\omega)$ are unitary matrices. The eigenvalues λ_i of the TRO are the squares of the singular values of $\mathbf{K}(\omega)$ and the eigenvectors are the columns of $\mathbf{V}(\omega)$. At this stage, we notice that if $\mathbf{E_H}(\omega)=E(\omega)\mathbf{I}$, [where $E(\omega)$ is the Fourier transform of the emitted signal and $\mathbf{I}$ is a unitary matrix] the SVD of $\mathbf{K}(\omega)$ is simply related to the SVD of $\mathbf{R}(\omega)$. In this paper, we assume that the target behaves as a discontinuity of compressibility. In this case, the number of "nonzero" eigenvalues is exactly the number of independent secondary sources given by the resolved scatterers present in the medium.[7] Eigenvectors are calculated in the time domain using an inverse Fourier transform, as described in Ref. 10.

III. EFFECT OF ABSORPTION

A. Theoretical approach

Let us consider the general ray-based formulation of the time dependent Green function between transducer i and the position of a single pointlike scatterer after multipath propagation (the response of the transducer i is not taken into account):

$$G_i(t)=\sum_r L_{r,i}\delta(t-\tau_{r,i}), \quad -1\leqslant L_{r,i}\leqslant 1, \qquad (3)$$

where $\delta(t)$ is equal to 1 at $t=0$ and is zero otherwise, $|L_{r,i}|$ is the loss of the rth arrival received by the ith transducer due to reflections and containing the effect of geometric spreading, and $\tau_{r,i}$ its time delay. Each nonzero temporal eigenvector $V(t)=\{V_i(t)\}_{i=1,N}$ of the TRO has the same multipath structure as $G_i(t)$ and can be written with the same convention as
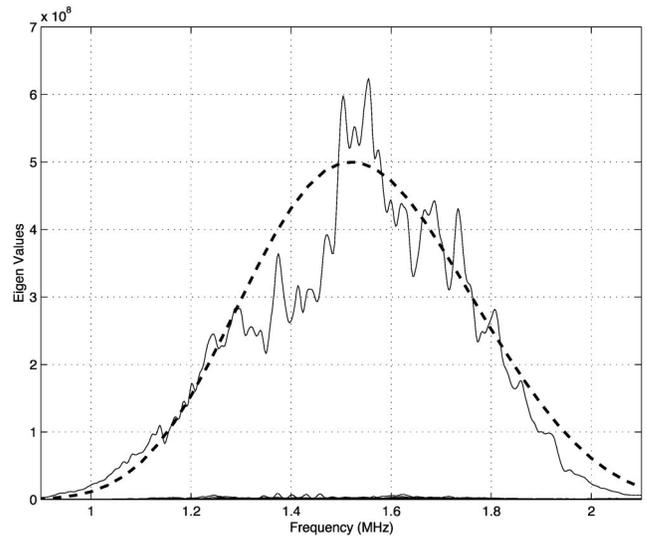
$$V_i(t)=\sum_r L_{r,i}E\delta(t+\tau_{r,i}),$$

FIG. 2. Experimental evolution of TRO eigenvalues in a rigid wave guide between 1 to 2 MHz. The dotted line represents the frequency response of the system.

where E is the maximum level supported by each source. The pressure at focus location and at focus time ($t=0$) obtained while transmitting $V(t)$ in the medium is

$$p_f(t=0)=\left(\sum_{i=1,N} G_i(t)\otimes V_i(t)\right)_{t=0}=\sum_{i=1,N}\sum_r L_{r,i}^2E. \qquad (4)$$

The time reversal process is affected by losses in the medium and especially at the interfaces. Thus, the losses at each reflection[15] result in an apodization of the virtual array given by the image theory.[1] Consequently, both vertical and horizontal resolutions are degraded.

Tanter et al.[16] proposed an amplitude compensation technique in the space domain for attenuated signals through the skull. In their case, only diffraction and absorption affected the propagation. Therefore, the compensation was performed at once for the entire signal received on each transducer. In our case of multipath propagation in a wave guide, the losses affect each arrival differently depending on the number of reflections. Thus, a specific technique has been developed in order to compensate strictly for this effect. In practice, the maximum level supported by each source is $\mathbf{E}$. Therefore, each component $V_i(t)$ of the eigenvector has to be transformed into $\widetilde{V}_i(t)$ by multiplying each arrival r by $\min_r(L_{r,i})/L_{r,i}^2$,

$$\widetilde{V}_i(t)=\sum_r \frac{\min_r(L_{r,i})}{L_{r,i}}E\delta(\tau_{r,i}+t).$$

This transformation provides a uniform amplitude wavefront near the focus, and as a consequence, better time compression and lower side lobes. In this case, the pressure at the focus and at time zero is

$$\widetilde{p}_f(t=0)=\left(\sum_{i=1,N} G_i(t)\otimes\widetilde{V}_i(t)\right)_{t=0}$$

$$=\sum_{i=1,N}\sum_r \min(L_{r,i})E. \qquad (5)$$

Therefore, the signal level at the focus will be very low because of the addition of the environmental losses. The best way to maximize $p_f(t=0)$ in order to maximize the signal to noise ratio at the target location is to normalize the amplitude of each arrival to $\mathbf{E}$,

$$\tilde{V}_i(t) = \sum_r E\,\delta(\tau_{r,i}+t).$$

One effect is to minimize virtual array apodization. In this case, the pressure at the focus is

$$\tilde{p}_f(t=0) = \left(\sum_{i=1,N} G_i(t)\otimes\tilde{V}_i(t)\right)_{t=0} = \sum_{i=1,N}\sum_r L_{r,i}E. \tag{6}$$

The pressure is maximized despite higher side lobes. The expected gain is closely related to both the number of array elements and the number of arrivals. In the following sections, we show experimentally the impact of this last weighting technique in comparison with the formal TRO eigenvectors.

In practice, separating the arrivals is not easy. Therefore, after matched filter processing, the envelope of each signal $\mathbf{V}_i(t)$ is calculated. Wave packets above a given threshold are isolated and normalized individually. As a consequence, most of the noise is not increased and the technique guarantees better resolution and better signal to noise ratio.

B. Experimental results

The results we present concern ultrasonic experiments within a water tank in the ultrasonic domain. The 40-element SRA has a 1.5 MHz central frequency and the array pitch is equal to 0.58 mm. For $F \gg D$, where F is the range and D the array aperture, the vertical and horizontal resolutions[15] in free space are $\mathfrak{R}_z \approx \lambda(F/D)$ and $\mathfrak{R}_x \approx 7\lambda(F/D)^2$. The configuration in the experiment gives $\mathfrak{R}_z \approx 14\lambda$.

Two different kinds of bottom are compared [Figs. 1(a) and (b)]. In both cases, the water depth is 27 mm and a single target (a wire of 0.04λ diameter, where λ is the wavelength) is placed in the water column at 330 mm range. For bottom (a), the lower boundary is a water/steel plane interface. The critical angle is very high and the losses of reflected arrivals are due to scattering and diffraction. Bottom (b) is a Plexiglas plate. Only a few bottom-reflected arrivals are above electronic noise because of a low critical angle and the large absorption.

The time reversal operator is measured and decomposed for bottom (a) and (b). In both cases, the first nonzero eigenvalue corresponds to the single target in the water column (Figs. 2 and 3). The temporal eigenvector obtained by an inverse Fourier transform is shown for each kind of bottom in Figs. 4 and 5. Indeed, it presents a series of resolved arrivals and one late unresolved arrival resulting from the interference between the direct rays and the lowest surface bottom reflected rays. The time dispersion of the eigenvectors depends on the absorption as well as on the number of resolved arrivals.

For bottom (a), the high critical angle of steel allows a large number of attenuated arrivals. Attenuation is due to
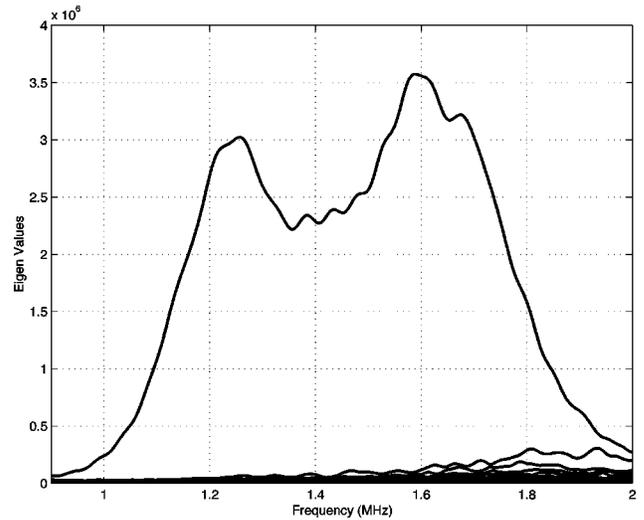

FIG. 3. Experimental TRO eigenvalues versus frequency in a highly absorbing wave guide made of Plexiglas.

scattering on the surface and on the bottom at each reflection. Therefore, the back propagation of this eigenvector gives a pressure profile focusing at the correct depth and range. The observed vertical resolution at the focus, while propagating the first eigenvector without any amplitude compensation, is about 4λ (dotted curve in Fig. 6 right). Therefore, in this case, the gain using the DORT method without amplitude compensation is about 3.5 and the equivalent array aperture in this wave guide (including apodization) is about 3.5 D. Thus, the gain in terms of horizontal resolution is about 12.

Amplitude compensation of the first eigenvector is carried out with the objective of increasing the acoustic pressure on the target as much as possible [Eq. (6)]. As expected, the signal to noise ratio gain is considerable, about 23 dB above the previous case. The vertical resolution is now approaching the diffraction limit value of $\lambda/2$ (solid curve in Fig. 6 right).

In the case of a high absorption level, as observed for the bottom (b), the benefit of amplitude compensation is affected by the low number of distinguishable arrivals above noise. The number of resolved arrivals is severely limited by
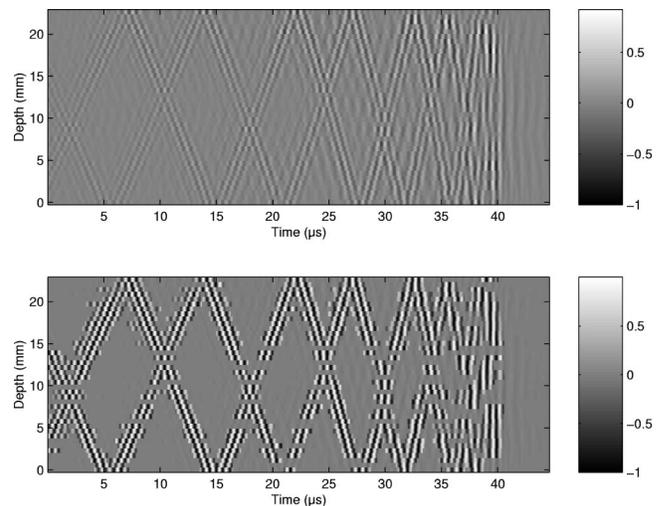

FIG. 4. First eigenvector versus time and depth measured in a perfect rigid wave guide (top) and after amplitude compensation (bottom).
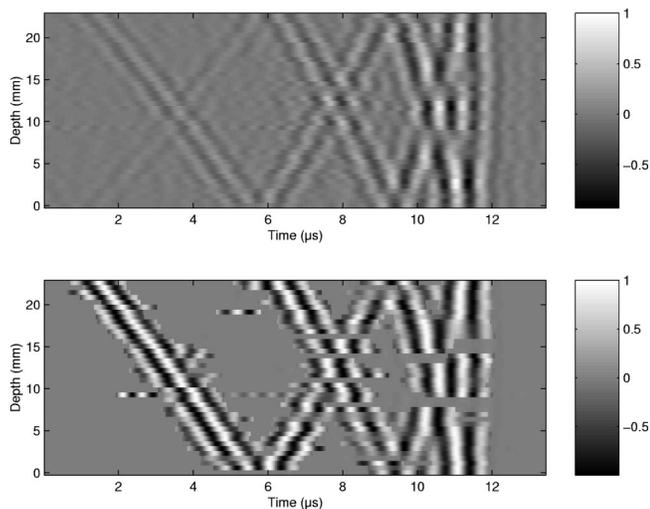
FIG. 5. First eigenvector versus time and depth measured in a wave guide with bottom absorption (top) and after amplitude compensation (bottom).

bottom absorption. However, as the amplitude compensation increases the contribution of the reflected arrivals, the vertical resolution remains good (Fig. 7). The signal to noise ratio at the target increases by 9 to 12 dB after amplitude compensation.

IV. REVERBERATION

Let us consider a single pointlike target in a shallow water environment when electronic noise and bottom reverberation occur. The bottom (c) is a steel base covered by a sandy layer that creates a realistic model of bottom reverberation [Fig. 1(c)]. The grain size of the sand is 0.5 ± 0.2 mm, which is around half a wavelength. For example, at 1 kHz in a real ocean it should correspond more to rocks than a sandy bottom. The reverberation curve in a monostatic configuration has been measured, Fig. 8. It shows that this
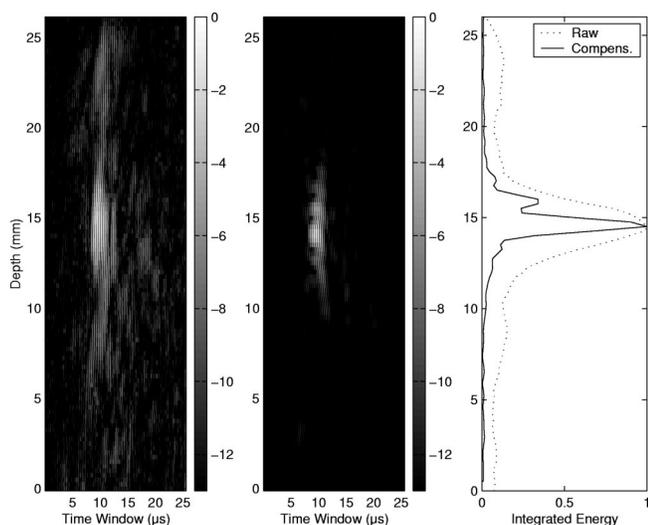

FIG. 6. Effect of amplitude compensation on the focus in a perfect rigid wave guide: the signals versus depth and time are measured while propagating the first eigenvector (left) and the compensated eigenvector (center). The integrated energy versus depth (right) shows the gain of the vertical resolution when amplitude is compensated (solid curve).
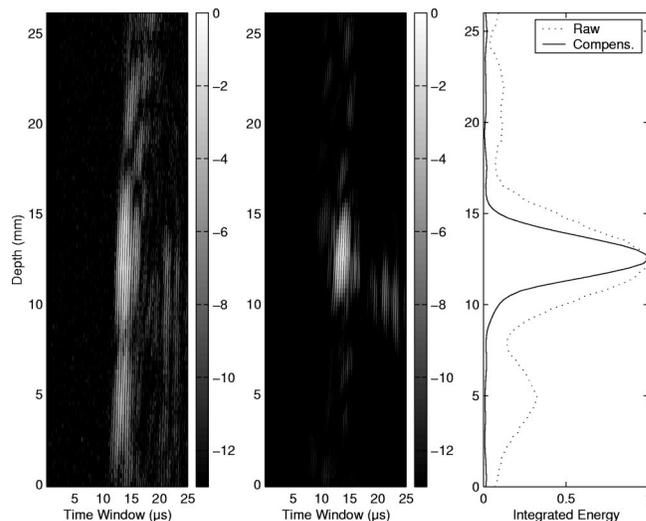

FIG. 7. Effect of amplitude compensation on the focus in an absorbing wave guide: the normalized signals versus depth and time are measured in dB while propagating the eigenvector (left), and the compensated eigenvector (center). The integrated energy versus depth (right) shows an improved vertical resolution when the amplitude is compensated (solid curve).

model provides a realistic representation of a reverberating and absorbing medium.

A. Ambient noise

In Figs. 2 and 3, one observes nonzero singular values, which are the signature of noise. The source level or the emission basis E_H used for the matrix acquisition will not affect the electronic and ambient noise eigenvalues. Nevertheless, the target eigenvalue levels also improve with the increase of the mean emitted energy. Therefore, the detection threshold should be improved in the same proportions.

B. Reverberation

In a theoretical work, Lingevitch et al.[14] extended the DORT method by modelling stochastic reverberation returns
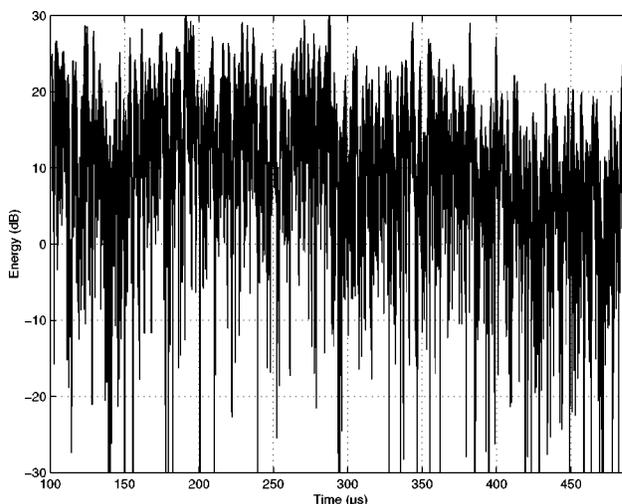

FIG. 8. Monostatic reverberation curve measured for the sand covered steel bottom: the reverberation is due to the sandy layer.
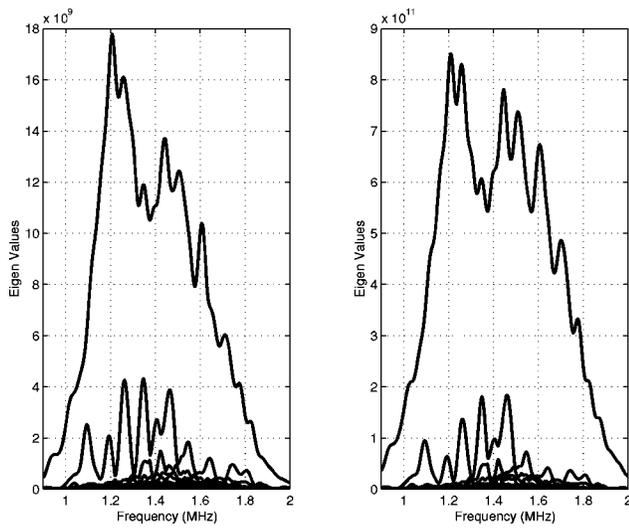
FIG. 9. Singular values versus frequency in a realistic ocean wave guide with absorption and reverberation while $\mathbf{E_H}$ is proportional to identity (left) and while $\mathbf{E_H}$ is proportional to the Walsh matrix (right).

FIG. 11. Range and depth distribution of acoustic energy around the target position by back propagation of the first eigenvector without (top) and with (middle) amplitude compensation and the second eigenvector with amplitude compensation (bottom).

from a rough sediment interface in an ocean wave guide. From their model, they demonstrated that the returned signals focus at the rough bottom interface.

In our experiment, the TRO is constructed in the presence of a single pointlike scatterer at 8.5 mm depth and at 330 mm range in a 25 mm deep sandy wave guide. Figure 9 shows the eigenvalues versus frequency when $\mathbf{E_H} = E(\omega)\mathbf{I}$ (canonical basis) and when $\mathbf{E_H} = E(\omega)\mathbf{H}$, where $\mathbf{H}$ is the Hadamard matrix (Walsh basis[14,17]). Additional nonzero eigenvalues appear in the curves. The magnitude of the singular values are N times higher in the Walsh basis than for the canonical emission (N being the number of array elements) because the source level of the system is N times higher in the Walsh basis. However, at each frequency, the relative magnitudes of the singular values are unchanged, meaning that the second singular value is not due to electronic noise but to an acoustic phenomenonlike reverberation. The differences of shape are unexpected since the Walsh basis is or-
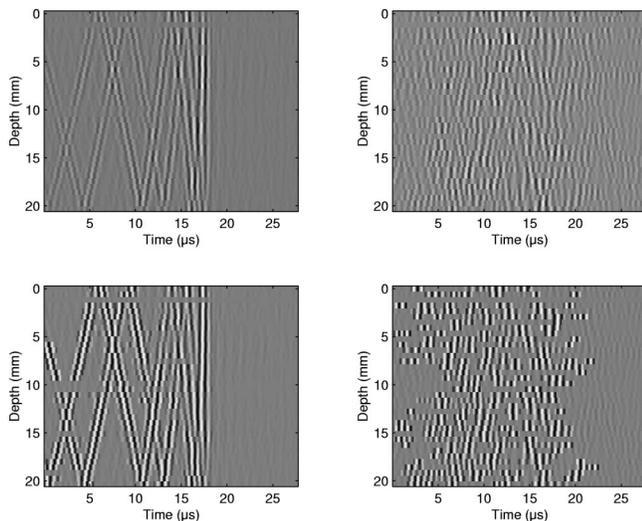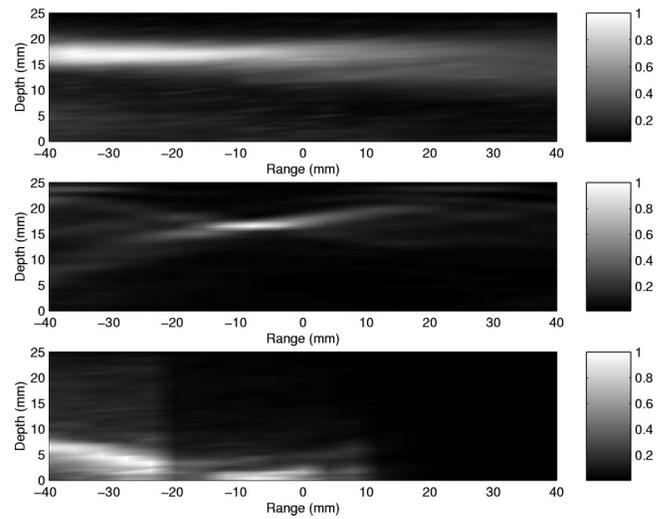

FIG. 10. First (left) and second (right) eigenvectors obtained in the realistic ocean wave guide (top) and after amplitude compensation (bottom).

thonormal and the singular values should be invariant to changes of bases. The coupling between the transducers, which occurs while all the channels are excited simultaneously, implies that the real emitted signals are not strictly orthogonal.

The time reversal operator is measured with bottom (c) using the canonical basis $\mathbf{E_H} = E(\omega)\mathbf{I}$. The two first eigenvectors are calculated (Fig. 10), compensated as described previously and back propagated. The pressure fields shown in Fig. 11 measured around the target position point out the vertical and horizontal resolution enhancement due to the amplitude compensation. The focusing is achieved on the sandy floor at the same range for the second eigenvector. These results confirm two important properties of the DORT method: first, the ability to take advantage of the environment, of the multipath propagation and of the used returned reverberation signals to increase signal to noise ratio on localized areas, second the ability to separate the reverberation from the target echo and consequently, the ability to focus selectively between reverberation and target.

This result is nontrivial because the spatial dispersion of the bottom speckle and the spatial focus zone are highly dependent on the time window length used in the time reversal operator. In fact, in order to increase the resolution, the method needs to take into account the whole time dispersion of echoes. Nevertheless, the time window must be limited because of the continuity of the target distribution in the bottom. In the experiment, the effective time window is 18 μs. As seen for the first dependent eigenvector associated with the pointlike target (left-hand side of Fig. 10), it allows about eight or nine reflected arrivals. The ranges of focus for both eigenvectors are the same and the focus sizes are both of the same order. The focus occurs at the closest range defined by the beginning of the time window. This can be explained by the greater attenuation of the return signal from longer ranges. The DORT method allows spatial selection on the bottom, and focus on its most reflective part. The characteristic size of the focus on the bottom is given by the

resolution of the complete system, composed of the array, the shallow water environment and the post-processing amplitude compensation.

V. CONCLUSION

These experiments show the ability of the DORT method to separate target echo from the reverberation signal. They also show the huge benefits of amplitude compensation for increasing the signal to noise ratio at the target and improving the vertical and horizontal resolution. The signal to noise ratio gain and the size of focus is directly connected to the array configuration, the environment characteristics and the method of amplitude compensation. Array configuration defines the basic resolution, the range limits of detection and the quality of focus by setting the level of side lobes. Multipath propagation associated with amplitude compensation provides a significant gain in the vertical and the horizontal resolutions and allows the possibility for focusing on the bottom.

ACKNOWLEDGMENTS

[1] P. Roux, B. Roman, and M. Fink, ''Time-reversal in an ultrasonic waveguide,'' Appl. Phys. Lett. **70**, 1811–1813 (1997).

[2] D. R. Jackson and D. R. Dowling, ''Phase conjugation in underwater acoustics,'' J. Acoust. Soc. Am. **89**, 171–181 (1991).

[3] W. A. Kuperman, T. Akal, C. Ferla, and D. R. Jackson, ''Phase conjugation in the ocean: Experimental demonstration of an acoustic time-reversal mirror,'' J. Acoust. Soc. Am. **103**, 25–40 (1998).

[4] W. S. Hodgkiss, H. C. Song, W. A. Kuperman, T. Akal, C. Ferla, and D. R. Jackson, ''Long-range and variable focus phase conjugation experiment in shallow water,'' J. Acoust. Soc. Am. **105**, 1597–1604 (1999).

[5] C. Prada, J. L. Thomas, and M. Fink, ''The iterative time reversal process: analysis of the convergence,'' J. Acoust. Soc. Am. **97**, 62–71 (1995).

[6] C. Prada and M. Fink, ''Eigenmodes of the time reversal operator: a solution to selective focusing in multiple target media,'' Wave Motion **20**, 151–163 (1994).

[7] C. Prada, S. Manneville, D. Spoliansky, and M. Fink, ''Decomposition of the time reversal operator: detection and selective focusing on two scatterers,'' J. Acoust. Soc. Am. **99**, 2067–2076 (1996).

[8] G. Bienvenu and L. Kopp, ''Optimality of high resolution array processing using the eigensystem approach,'' IEEE Trans. Acoust., Speech, Signal Process. **31**, (1993).

[9] R. O. Schmidt, ''Multiple emitter location and signal parameter estimation,'' IEEE Trans. Antennas Propag. **AP-34**, 276–281 (1986).

[10] N. Mordant, C. Prada, and M. Fink, ''Highly resolved detection and selective focusing in a waveguide using the D.O.R.T. method,'' J. Acoust. Soc. Am. **105**, 2634–2642 (1999).

[11] C. Prada, T. Folégot, N. Mordant, and M. Fink, ''Time reversal operator decomposition in a ocean wave guide,'' Proceedings of the 5th Underwater Acoustics Days, Brest, Session 8-23, France, 2000.

[12] T. Yokoyama, T. Kikuchi, T. Tsuchiya, and A. Hasegawa, ''Detection and selective focusing on scattering using decomposition of time reversal operator method in pekeris waveguide model,'' Jpn. J. Appl. Phys. **40**, (2001).

[13] J. S. Kim, H. C. Song, and W. A. Kuperman, ''Adaptive time-reversal mirror,'' J. Acoust. Soc. Am. **109**, 1817–1825 (2001).

[14] J. F. Lingevitch, H. C. Song, and W. A. Kuperman, ''Time reversed reverberation focusing in a waveguide,'' J. Acoust. Soc. Am. **11**, 2609–2614 (2002).

[15] M. Born and E. Wolf, *Principles of Optics* (Academic, New York, 1970).

[16] M. Tanter, J. L. Thomas, and M. Fink, ''Focusing and steering through absorbing and aberrating layers: Application to ultrasonic propagation through the skull,'' J. Acoust. Soc. Am. **103**, 2403–2410 (1998).

[17] S. Azzaretti, D. Dotti, R. Lombardi, and D. Rossi, ''Echo-graphic images enhanced through walsh functions,'' IEEE Ultrasonics Symposium, 1997, pp. 675–678.